International Journal of Research in Engineering and Innovation (IJREI)
journal home page: http://www.ijrei.com
ISSN (Online): 2456-6934

ORIGINAL ARTICLE

Effect of nanoparticles and multipass friction stir processing on microstructure and mechanical properties of AA7475

Vikas Kumar, Promila, Amit Gupta

Department of Mechanical Engineering, Geeta Engineering College, Panipat India

Article Information

Received: 17 March 2023
Revised: 6 April 2023
Accepted: 21 May 2023
Available online: 28 May 2023

Keywords:

Mechanical properties
Microstructure
Microhardness
Multipass
Friction stir processing

Abstract

The base metal, AA7475, initially contained nanoparticles of SiC within a coarse dendritic structure. The multipass FSP (MPFSP) process successfully broke these coarse and dendritic clusters, resulting in a homogenous microstructure in the stir zone. This inhibition led to a continual reduction in grain size. The presence of SiC reinforcement particles also played a role in imbvproving the microstructure and tensile properties of the MPFSP/SiC composite. The optimal process parameters for MPFSP/SiC on AA7475 were identified as a rotational tool speed of 1500 rpm, welding speed of 40 mm/min, and a tilt angle of 2°. As the number of FSP passes increased, the agglomeration of SiC particles reduced, further enhancing the dispersion. Before MPFSP/SiC, the base metal AA7475 exhibited a tensile strength of 410±5 MPa and a % strain of 10.83±0.3. However, after MPFSP/SiC, the tensile strength increased with the number of FSP passes. The highest tensile strength of 521±8 MPa was observed after the 5th pass of FSP. This increase in tensile strength was attributed to the presence of fine grains formed through the DRX mechanism during the MPFSP process.

1. Introduction

The friction stir processing (FSP) with nanoparticles provides an overview of the significance and challenges associated with fabricating aluminum matrix nanocomposites (AMNCs) and highlights the use of FSP as a promising fabrication method [1-3]. It also emphasizes the importance of incorporating various reinforcement particles to enhance the tensile properties of AMNCs. AMNCs are gaining popularity in defense, automotive, and aerospace engineering applications due to their high strength-to-weight ratio [4-9]. However, joining AMNCs using fusion welding techniques often leads to issues such as porosity, coarse microstructure, segregation, and decomposition of nanoparticles [10, 11]. In contrast, FSP offers advantages over fusion processes as it operates at lower temperatures and allows for severe plastic mixing, reducing these issues. Researchers have used different reinforcement particles to improve the tensile properties of AMNCs and achieve a homogeneous distribution of nanoparticles [12-15]. For example, Al_2O_3 reinforcement particles were uniformly disseminated in an AMNC, and a grain size of 72nm was observed in the 4th pass of FSP. Various other reinforcement particles, such as SiC, have also been used to fabricate AMNCs with superior wear and tensile properties compared to the base metal. FSP has been widely employed to enhance the tensile strength of aluminum alloys using nanoparticles [16, 17]. SiC reinforcement particles have been extensively studied for their ability to improve the microstructure and ultimate tensile strength (UTS) of AMNCs [18-20]. Additionally, researchers have explored the feasibility of incorporating FSP in the fabrication of different aluminum alloys using SiC reinforcement particles. The passage also mentions the

Corresponding author: Vikas Kumar
Email Address: vikaskumar03071997@gmail.com
https://doi.org/10.36037/IJREI.2023.7301.

combination of tungsten inert gas (TIG) welding and FSP to improve the microstructure and UTS of dissimilar TIG welded joints. This approach has shown promising results [20-24]. Fabricating reinforcement composites remains a challenge, but FSP has emerged as a promising method for modifying the microstructure of AMNCs. It allows for a homogenized distribution of second-phase particles in grain-refined AMNCs [25-28]. In recent years, research has focused on the FSP of aluminum alloys with various nanoparticles, including B4C, TiB2, TiC, and Mg_2Si. SiC is highlighted as an attractive nanoparticle for AMNCs due to its resistance to shocks, stability in aggressive environments, high hardness, and melting point. SiC reinforcement effectively enhances the wear, microstructure, and tensile properties of AMNCs. The passage also mentions the mechanisms that contribute to the improved properties of AMNCs, including dislocation strengthening, grain boundary strengthening, and Orowan strengthening [29-34].

In the present work, the influence of reinforcement particles on the microstructure, particle distribution, microhardness value, and tensile properties of MPFSP of AA7475 was investigated. Overall, the passage highlights the importance of reinforcement particles, FSP, and microstructural modifications in enhancing the properties of AMNCs, particularly in terms of microstructure, particle distribution, microhardness, and tensile strength.

2. Materials and Methods

In the present work, the fabrication of MPFSP with Al_2O_3 reinforcement particles was conducted using AA7475 as the parent metal. The chemical composition of AA7475 was demonstrated in table 1. The starting material was cut into plates with dimensions of 6.2×80×180 mm using an EDM (Electrical Discharge Machining) machine. A groove with dimensions of 3.2×2.5×175 mm was created on the base metal, and this groove was filled with Al_2O_3 reinforcement particles. A pin-less tool was utilized to close the groove, and the MPFSP process was carried out with a tool rotational speed (TRS) of 500 to 1500 rpm and a welding speed (WS) of 40 mm/min. To ensure proper alignment, a fixture was employed during the fabrication process to prevent misalignment of the base metal, as shown in Fig. 1. The number of FSP passes varied from one to five, while the axial force and tilt angle were maintained at 7.5 KN and 2°, respectively. Temperature variations during MPFSP were monitored using an infrared thermometer mounted on the FSP machine, and the peak temperature of the MPFSP samples ranged from 434 to 462°C.

Table 1: Chemical composition of AA7475

Material	Zn	Mg	Si	Cr	Fe	Mn	Cu	Al
AA7475	5.82	1.75	0.11	0.025	0.085	0.057	1.97	Bal

The square pin profile, made of H13 tool steel and having a hardness of 434 HV, was used during the process. Following fabrication, all MPFSP samples were allowed to cool at room temperature. After the MPFSP process, the processed specimens underwent polishing with emery paper of varying grades (600 to 2200) to achieve a smooth surface for microstructure testing. Tensile specimens were prepared according to the ASTM E8 standard [35]. The fractured surfaces of the tensile-tested specimens were examined using a scanning electron microscopy (SEM) machine. The microstructure of the MPFSPed specimens was characterized using optical machine. The microstructure samples were polished with emery paper and etched with Keller's reagent (8 ml HNO_3, 6 ml HCl, 4 ml HF, and 82 ml water) for 10 seconds, following the ASTM E384 standard. Hardness testing was performed using a Vickers hardness machine with a load of 150 grams for 10 seconds at ambient temperature.

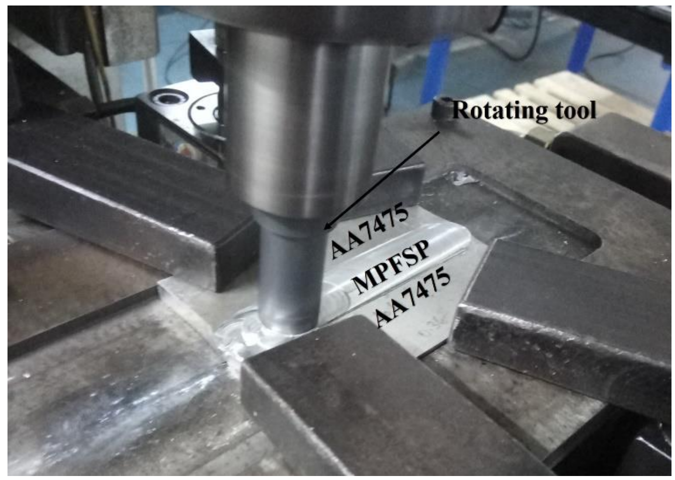

Figure 1: Multipass friction stir processing

3. Results and Discussion

3.1 Microstructure analysis

The optical microstructure (OM) of multipass FSP as shown in Fig. 2. The processed region revealed distinct regions, namely the Heat-Affected Zone (HAZ), Thermo-Mechanically Affected Zone (TMAZ), and Stir Zone (SZ). No internal defects were observed in any of the samples. The microstructure of the SZ was strongly influenced by the heat input. Compared to the HAZ and TMAZ regions, the SZ exhibited finer and equiaxed grain structures, which can be attributed to intense plastic deformation and frictional heat during the FSP process. The heat input, along with the annealing effect and dynamic recrystallization (DRX), led to the nucleation of new grains, resulting in finer grain sizes and inhibiting grain boundary sliding during FSP [36-42]. Fig. 2a displays the OM of the MPFA of AA7475. The base metal exhibited coarse and elongated grain structures (139±5 μm). The one-pass (1P) FSP process induced severe plastic deformation and DRX, resulting in a refined microstructure in the SZ. The grain size of the base metal and MPFSP samples was analyzed using Image J software. The grain sizes for 1P, 3P, and 5P FSP were measured to be 25±7 μm, 7±4 μm, and 2±3 μm, respectively.

The grain structure of the as-cast material gradually improved in the HAZ, TMAZ, and SZ regions during 1P FSP, and the grain structure in the SZ continued to improve with increasing FSP passes [43]. During the MPFSP process, the microstructure was further refined. The SZ exhibited a fine and equiaxed grain structure in the thickness direction, which was influenced by the processing temperature of the SZ [44-48]. Fig. 2a-b illustrates the microstructure of the as-cast AA7475 with Al_2O_3 reinforcement particles subjected to different FSP passes. The primary Al_2O_3 particles were homogenized and refined as the number of FSP passes increased. The coarse grain structure of the base material was reduced after 1P FSP. The reinforcement particles in the SZ were further fragmented and dispersed after 2P FSP due to material mixing and dispersion. Substantial and progressive segmentation of the reinforcement particles occurred after 4P and 5P FSP. With an increase in FSP passes, the area fraction of reinforcement particles increased, indicating a relationship between particle dispersion and FSP passes [49]. The 4P and 5P FSP exhibited a more uniform grain structure due to fine grains formed through DRX, influenced by Zener-Hollomon parameters [50]. Therefore, a homogeneous and fine microstructure was achieved during MPFSP, which resulted in improved mechanical properties. The 5P FSP exhibited higher mechanical properties compared to 1P, 2P, 3P, and 4P FSP/Al_2O_3 [51, 52]. In 1P FSP, the bonding between the surrounding Al-alloy and agglomerated particles was found to be the weakest. However, with an increase in FSP passes, these deficiencies were eliminated. During the plunging stage, the rotating FSP tool compressed the reinforcement particles and the parent metal. When the tool pin and reinforcement particles came into contact, the reinforcement particles transferred to the side faces.

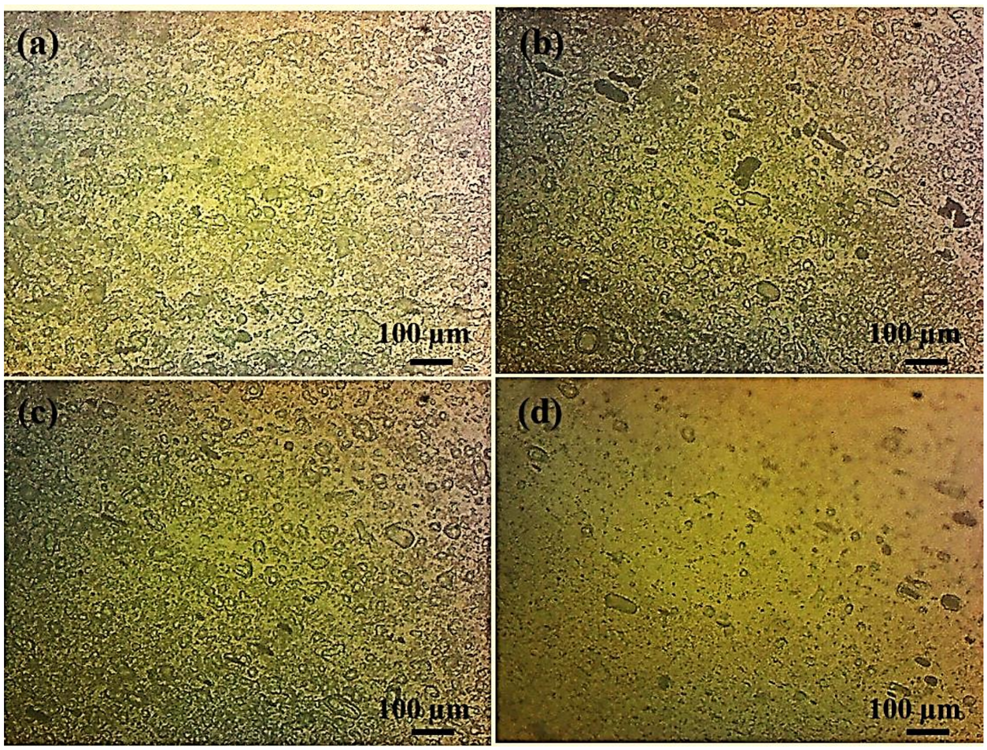

Figure 2: Optical microstructure of multipass FSP of AA7475, (a) 1P FSP, (b) 2P FSP, (c) 3P FSP, (d) 5P FSP

3.2 Tensile strength

Table 2 shows the UTS values of the MPFSP/Al_2O_3 composite of AA7475. The maximum and minimum joint efficiency was found to be 126.56%, and 104.09% for 5th pass FSP and single pass FSP at TRS of 1500 rpm and 500 rpm respectively compared to the parent metal. The percentage strain and hardness of the MPFSPed specimens exhibited a similar trend, indicating that increasing the number of FSP passes led to significantly finer Al_2O_3 nanoparticles and improved mechanical properties. This observation is consistent with findings reported by other researchers [53, 54]. Fig. 3 illustrates the stress-strain diagram of the base metal and MPFSP/Al_2O_3 composite of AA7475. The presence of reinforcement particles significantly influenced the hardness and UTS. As the number of FSP passes increased, the UTS of the MPFSP/Al_2O_3 composite of AA7475 increased from 410 to 525 MPa. All the tensile test specimens were fractured at the HAZ and TMAZ regions, which has also been reported by other researchers [55]. The UTS of the MPFSP/Al_2O_3 composite was higher than that of the base material due to the improved strength and ductility resulting from the thermal properties of the parent material. Reducing dislocation and the driving force at grain boundaries of the Aluminum Matrix nano-composites (AMNCs) during axial loading was essential [56, 57].

Table 2: Mechanical Properties of FSPed joint AA7475

Run	TRS (rev/min)	FSP pass	TS (mm/min)	UTS (MPa)	% Strain	Joint efficiency (%)	Hardness (HV)
1	500	1	40	428.83	11.56	104.09	159
2	500	3		439.62	13.54	106.7	145
3	500	5		443.59	12.96	107.66	168
4	1000	1		435.21	14.56	105.63	164
5	1000	3		459.37	13.53	111.49	157
6	1000	5		478.94	14.84	116.24	138
7	1500	1		464.57	14.29	112.75	125
8	1500	3		484.26	15.36	117.53	119
9	1500	5		521.44	17.89	126.56	134

The base material exhibited a UTS of 410±5 MPa and a percentage strain of 10.83±0.3. The UTS values of 1P, 3P, and 5P FSP were measured as 464.57±3 MPa, 484.26±4 MPa, and 521.44±5 MPa, respectively at TRS of 1500 rpm, influenced by the presence of strain-free grains during microstructure refinement and DRX. The reinforcement particles contribute to the strengthening mechanism by acting as nucleation sites for dislocation production due to strain divergence and plastic constraint [58]. The equiaxed and fine-grain structures with a large fraction of High-Angle Grain Boundaries (HAGBs) achieved through MPFSP have a significant impact on the UTS. The enhancement of UTS in the MPFSP/Al_2O_3 composite is primarily attributed to the significant grain refinement. Moreover, the substantial fraction of HAGBs indicates a high misorientation between neighboring grains, providing additional obstacles and increased resistance against grain boundaries interrupted by dislocations, thereby contributing to grain boundary strengthening [59]. Additionally, the presence of dispersed minor second-phase crystals acts as dominant barrier to dislocation motion, further increasing the UTS of the MPFSP region [60]. Grain refinement helps improve the compatibility of neighboring grains and thus enhances the percentage strain. The uniform distribution of fine second-phase crystals contributes to the improvement of the percentage strain.

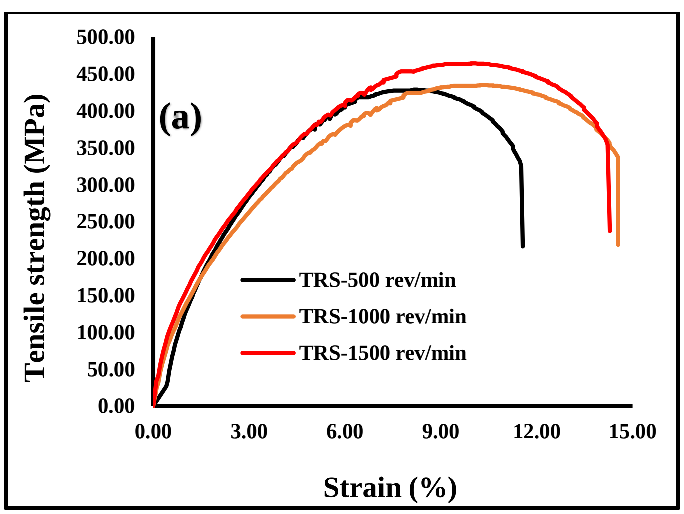

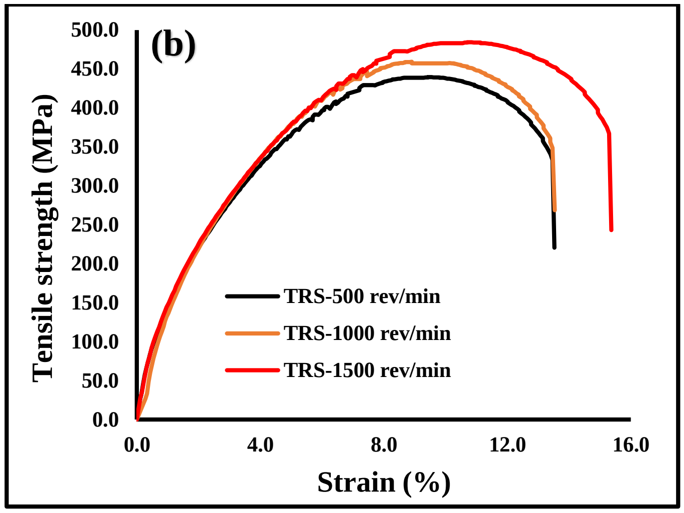

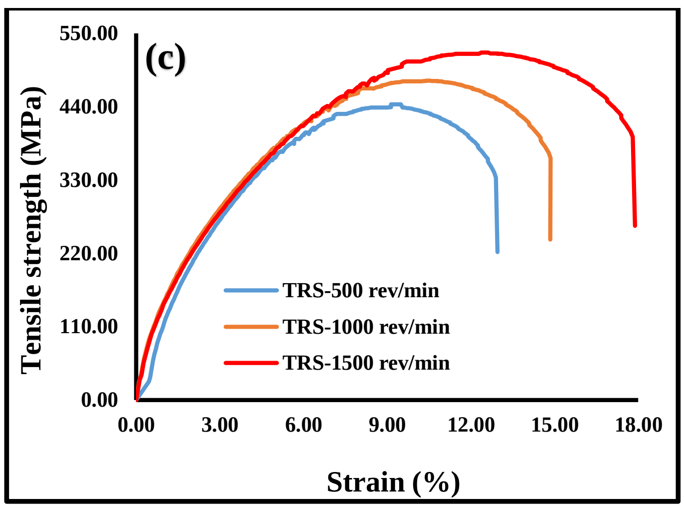

Figure 3: Stress-strain curve of Al-7475/Al_2O_3 subjected to MPFSP, (a) 1P FSP, (b) 3P FSP, (c) 5P FSP

3.3 Microhardness analysis

Fig. 4 presents the hardness profiles of the MPFSP/Al_2O_3 composite of AA7475. The continuous improvement in hardness was achieved with increasing FSP passes due to factors such as fine grain sizes, higher dislocation density, and the presence of Al_2O_3 nanoparticles. The as-cast AA7475 exhibited a hardness value of 128 HV, characterized by coarse and elongated grains. However, the presence of a fine and equiaxed grain structure formed by uniformly distributed Al_2O_3 particles and DRX led to an average hardness of 168 HV in the 5th FSP pass at TRS of 500 rpm.

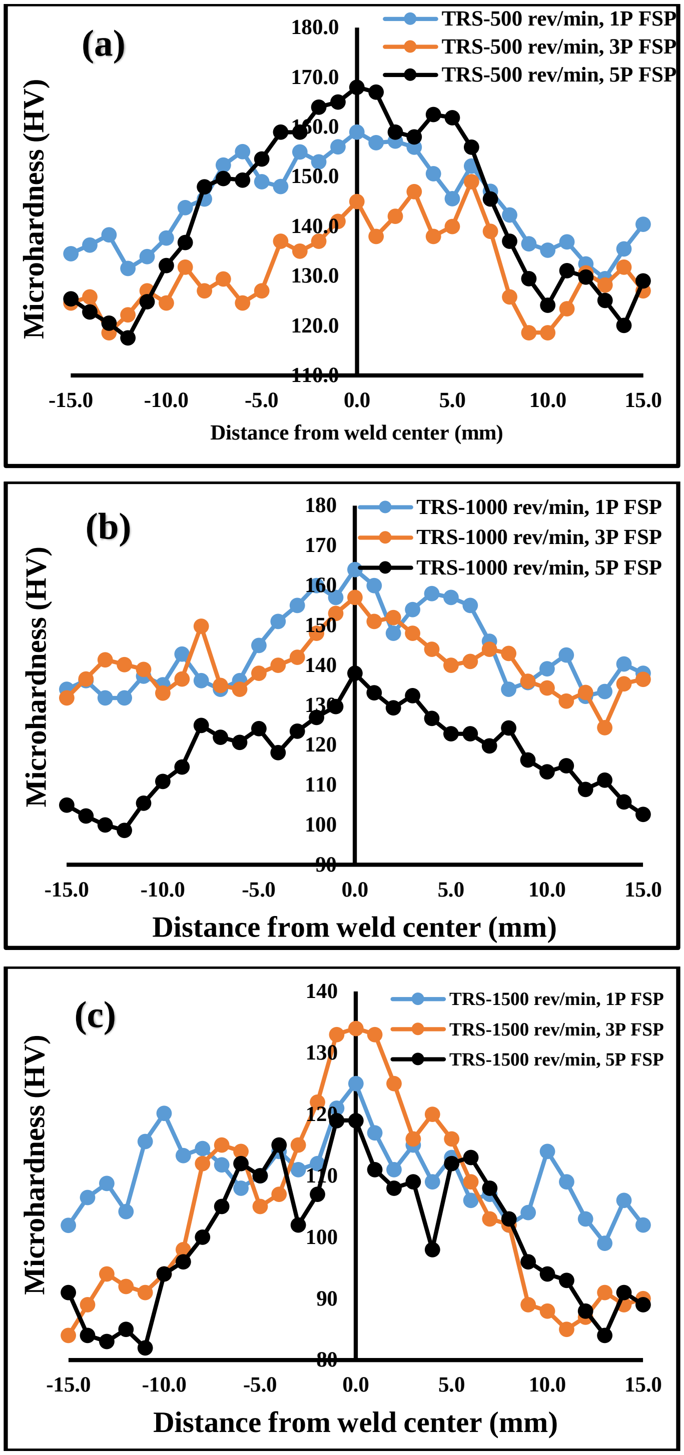

Figure 4: Variation of microhardness of multipass FSP/Al_2O_3 of AA7475, (a) TRS-500 rev/min, (b) TRS-1000 rev/min (c) TRS-1500 rev/min

The hardness distribution was uneven in the HAZ and TMAZ regions, which can be attributed to the inhomogeneous microstructure of the MPFSP/Al_2O_3 composite. The Hall-Petch relationship, combined with the presence of hard reinforcing Al_2O_3 nanoparticles, suggests that the fine grains in the Aluminum Matrix Nano Composites (AMNCs) are related to the temperature distribution in the welded region. The minimal fluctuation in the hardness of the FSPed samples was due to the intermixing and dispersion of the parent material and Al_2O_3 reinforcement particles. The strengthening effect of the reinforcement particles was stronger in the 4P FSP compared to the 1P FSP, attributed to the fine grains and hard nature of the Al_2O_3 phase, following the material mixing rule. In the MPFSP/Al_2O_3 composite of AA7475, the heat generated during DRX and intense plastic strain led to the formation of equiaxed and fine grains in the stir zone, causing mechanical rupture of the inherent grain boundaries. The fragmentation of Al_2O_3 reinforcement particles during MPFSP allowed for grain boundary migration [61]. Accumulated reinforcement particles acted as preferred sites for new grains after DRX. Therefore, the increase in hardness during MPFSP can be attributed to a combination of dispersion strengthening, reinforcement particles, and grain refinement. The hardness value in the stir zone (SZ) was higher than in the heat-affected zone (HAZ) and thermo-mechanically affected zone (TMAZ) due to the fine grain size present. The lowest hardness was observed in the HAZ, where the coarsening of strengthening precipitates and Guinier-Preston zones were absent.

3.4 Fractography

In single-pass FSP, the redistribution and refinement of particles occurred, leading to the removal of the dendritic structure. This redistribution prevented inter-dendritic crack propagation and disseminated the cracks through the aluminum base. As a result, the aluminum base zone exhibited ductility, leading to improved ductility of the material. Micro dimples were observed on the ruptured surface, as shown in Fig. 5. The presence of cleavage and dimples indicated the heterogeneous dispersion of agglomerated Al_2O_3 nanoparticles in the Aluminum Matrix NanoComposites (AMNCs). In the first and second FSP passes, the occurrence of cleavage and dimples suggested a ductile fracture behavior. In the 5th FSP pass, fine and homogeneous dimples were more prominent compared to other FSP passes, which are characteristic features of ductile fracture. During the tension test, a cup-cone fracture was observed at a 45° angle to the tensile axis along the periphery of the specimens, indicating ductile fracture [62]. Single-pass FSP/AAl_2O_3 samples exhibited honeycomb-like dimples, indicating agglomerative and microporous ductile fractures. In the 3rd FSP pass, equiaxed and fine dimples were observed without cleavage facets, indicating virtuous ductile fracture behavior of the AMNCs. However, in the MPFSP/Al_2O_3samples, fractures occurred in the thermo-mechanically affected zone (TMAZ) and heat-affected zone (HAZ) due to material softening and the presence of a coarse grain structure, consistent with previous research [63, 64]. The fractography of the samples was primarily determined by the coalescence of micro-voids, nucleation, and dimples. With an increase in the number of FSP passes, the dimples became smaller in the MPFSP of aluminum alloys. The increase in strength and ductility after precipitation hardening can be attributed to the presence of more homogenous and uniform dimples, as illustrated in Fig. 5.

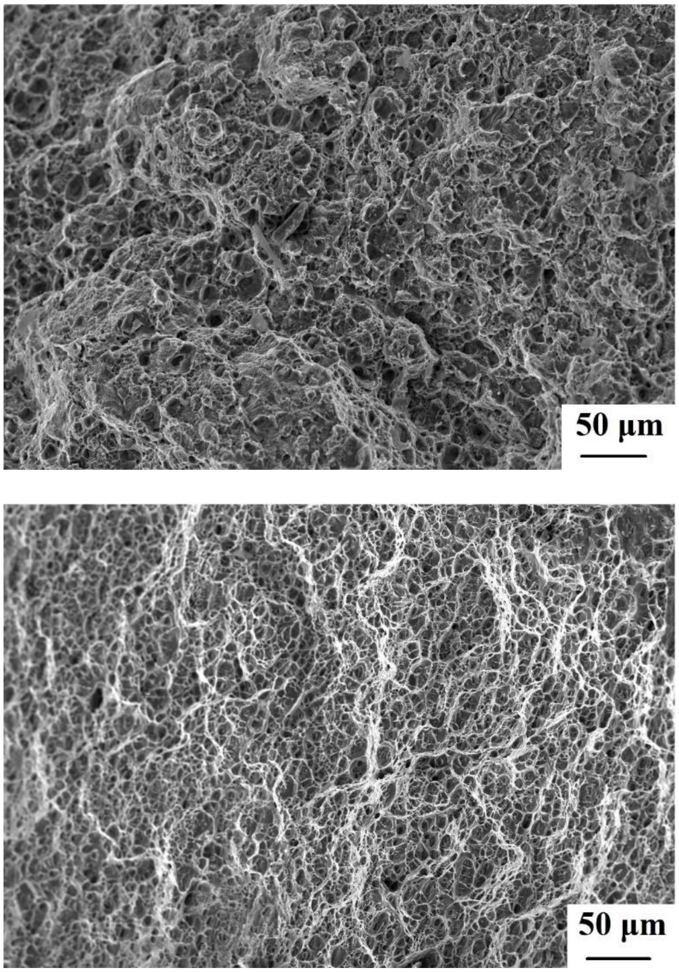

Figure 5: Fractography of AA7475/Al_2O_3 composite, (a) one pass, (b) five passes

3.5 Conclusions

The investigation on the effect of Al_2O_3 reinforcement particles and multi-pass friction stir processing (MPFSP) on the mechanical properties and microstructure of as-cast AA7475 resulted in the following conclusions:

- The fabrication of homogeneously dispersed Al_2O_3 reinforcement particles in the fine-grained Aluminum Matrix NanoComposites (AMNCs) was successfully achieved by the 5th FSP pass. The addition of Al_2O_3reinforcement particles led to a Zener pinning effect, resulting in a fine grain structure and improved mechanical properties.
- The base material exhibited a UTS of 410±5 MPa and a percentage strain of 10.83±0.3. The UTS values of 1P, 3P, and 5P FSP were measured as 464.57±3 MPa, 484.26±4 MPa, and 521.44±5 MPa, respectively at TRS of 1500 rpm, influenced by the presence of strain-free grains during microstructure refinement and DRX.
- With an increase in the number of FSP passes, the grain size of the composite was modified through particle-induced pinning. The fragmented Al_2O_3 nanoparticles provided resistance to grain growth, resulting in the retention of dynamically recrystallized (DRX) grains in the AMNCs.
- The combination of dispersion strengthening and grain refinement strengthening in the 5th FSP pass significantly contributed to the improved tensile properties of the composite. In the as-cast AA7475, fracture was controlled by pre-existing pores and particle clustering at the grain boundaries. However, in the 5th FSP pass, fracture was dominated by the coalescence of micro voids caused by dislocation accumulation at the interfaces between aluminum and Al_2O_3.
- The as-cast AA7475 exhibited a hardness value of 128 HV, characterized by coarse and elongated grains. However, the presence of a fine and equiaxed grain structure formed by uniformly distributed Al_2O_3 particles and DRX led to an average hardness of 168 HV in the 5th FSP pass at TRS of 500 rpm. The hardness distribution was uneven in the HAZ and TMAZ regions, which can be attributed to the inhomogeneous microstructure of the MPFSP/Al_2O_3 composite.

References

[1] Khodabakhshi, F., Nosko, M., Gerlich, A.P., 2018. Effect of graphene nano-platelets (GNPs)on the microstructural characteristics and textural development of an Al-Mg alloy during friction-stir processing. Surf. Coat. Technol. 335, 288-305.

[2] Husain Mehdi, Arshad Mehmood, Ajay Chinchkar, Abdul Wahab Hashmi, Chandrabhanu Malla, Prabhujit Mohapatra, Optimization of process parameters on the mechanical properties of AA6061/Al2O3 nanocomposites fabricated by multi-pass friction stir processing, Materials Today: Proceedings, 56 (4), 1995-2003, 2021, https://doi.org/10.1016/j.matpr.2021.11.333.

[3] Dolatkhah, A., Golbabaei. P., Givi, M.K.B, Molaiekiya, F., 2012. Investigating effects of process parameters on microstructural and mechanical properties of Al5052/SiC metal matrix composite fabricated via friction stir processing. Mater. Des. 37, 458–464.

[4] Sumit Jain, R.S. Mishra, Husain Mehdi, Influence of SiC Microparticles and Multi-Pass FSW on Weld Quality of the AA6082 and AA5083 Dissimilar Joints. Silicon (2023). https://doi.org/10.1007/s12633-023-02455-x

[5] Shaurya Bhatnagar, Gaurav Kumar, Husain Mehdi, Mukesh Kumar, Optimization of FSW parameters for enhancing dissimilar joint strength of AA7050 and AA6061 using Response Surface Methodology (RSM), materials today proceedings, 2023. https://doi.org/10.1016/j.matpr.2023.04.144.

[6] Sharifitabar, M., Sarani, A., Khorshahian, S., Shafiee, A. M., 2011. Fabrication of 5052Al/Al_2O nanoceramic particle reinforced composite via friction stir processing route. Mater. Des. 32, 4164–4172.

[7] Shivraman Thapliyal Dheerendra Kumar Dwivedi, Microstructure evolution and tribological behavior of the solid lubricant based surface composite of cast nickel aluminum bronze developed by friction stir processing, Journal of Materials Processing Technology; 2016: 238, 30-38.

[8] Husain Mehdi, Anil Kumar, Arshad Mahmood, Manoj Saini, Experimental Analysis of Mechanical Properties of Composite Material

Reinforced by Aluminium-Synthetic Fibers, International Journal of Mechanical Engineering, 2 (4), 59-69, 2014.

[9] Sipokazi Mabuwa, Velaphi Msomi, Husain Mehdi, Tiyamike Ngonda, A study on the metallurgical characterization of the longitudinally sampled friction stir processed TIG welded dissimilar aluminum joints, Journal of Process Mechanical Engineering, 2023, https://doi.org/10.1177/09544089231169589.

[10] Barmouz M, Besharati Givi MK. Fabrication of in situ Cu/SiC composites usingmulti-pass friction stir processing: evaluation of microstructural, porosity,mechanical and electrical behavior. Composites Part A 2011;42:1445–53.

[11] Sipokazi Mabuwa, Velaphi Msomi, Husain Mehdi, Kuldeep Kumar Saxena, Effect of material positioning on Si-rich TIG welded joints of AA6082 and AA8011 by friction stir processing, Journal of Adhesion Science and Technology, 2022. https://doi.org/10.1080/01694243.2022.2142366.

[12] Shivraman Thapliyal & Dheerendra Kumar Dwivedi (2018) Barium titanate reinforced nickel aluminium bronze surface composite by friction stir processing, Materials Science and Technology. 2018; 34(3):366-377.

[13] Husain Mehdi, R.S. Mishra, Mechanical properties and microstructure studies in Friction Stir Welding (FSW) joints of dissimilar alloy- a review, Journal of Achievements in Materials and Manufacturing Engineering, 77 (1), 31-40, (2016).

[14] Barmouz M, Asadi P, Besharati Givi MK, Taherishargh M. Investigation ofmechanical properties of Cu/SiC composite fabricated by FSP: effect of SiCparticles' size and volume fraction. Mater Sci Eng A 2011;528:1740–9.

[15] Abdul Wahab Hashmi, Husain Mehdi, Sipokazi Mabuwa, Velaphi Msomi & Prabhujit Mohapatra, Influence of FSP Parameters on Wear and Microstructural Characterization of Dissimilar TIG Welded Joints with Si-rich Filler Metal. Silicon, 14, 11131–11145, 2022. https://doi.org/10.1007/s12633-022-01848-8

[16] Abdul Wahab Hashmi, Husain Mehdi, R. S. Mishra, Prabhujit Mohapatra, Neeraj Kant & Ravi Kumar, Mechanical Properties and Microstructure Evolution of AA6082/Sic Nanocomposite Processed by Multi-Pass FSP. Transactions of the Indian Institute of Metals, (2022), 75, 2077–2090. https://doi.org/10.1007/s12666-022-02582-w.

[17] Abdellah Nait Salah, Sipokazi Mabuwa, Husain Mehdi, Velaphi Msomi, Mohammed Kaddami, Prabhujit Mohapatra, Effect of Multipass FSP on Si-rich TIG Welded Joint of Dissimilar Aluminum Alloys AA8011-H14 and AA5083-H321: EBSD and Microstructural Evolutions. Silicon, 14, 9925–9941, 2022.https://doi.org/10.1007/s12633-022-01717-4.

[18] M. Barmouz, M.K. Besharati Givi, J. Seyfi, On the role of processing parameters in producing Cu/SiC metal matrix composites via friction stir processing: investigating microstructure, microhardness, wear and tensile behavior, Mater. Charact. 62 (2011) 108–117.

[19] G.Q. Huang, J. Wu, W.T. Hou, L.H. Shah, A.R.H. Midawi, A.P. Gerlich, Y. F. Shen, F.Q. Meng, Microstructural evolution and mechanical behavior of powder metallurgy based SiC/Al–Mg-Sc-Zr nanocomposite subjected to multi-pass friction stir processing, Materials Science & Engineering A, 806 (2021) 140831.

[20] Husain Mehdi, R.S. Mishra, Investigation of mechanical properties and heat transfer of welded joint of AA6061 and AA7075 using TIG+FSP welding approach, Journal of Advanced Joining Processes, 1, 100003, (2020) https://doi.org/10.1016/j.jajp.2020.100003.

[21] Husain Mehdi, R.S. Mishra, Effect of Friction Stir Processing on Microstructure and Mechanical Properties of TIG Welded Joint of AA6061 and AA7075, Metallography, Microstructure, and Analysis, 9, 403–418 (2020). https://doi.org/10.1007/s13632-020-00640-7

[22] Husain Mehdi, R.S. Mishra, Study of the influence of friction stir processing on tungsten inert gas welding of different aluminum alloy. SN Applied Science, 1, 712 (2019). https://doi.org/10.1007/s42452-019-0712-0.

[23] Husain Mehdi, R.S. Mishra, Effect of friction stir processing on mechanical properties and heat transfer of TIG welded joint of AA6061 and AA7075, Defence Technology, 17 (3), 715-727 (2021). https://doi.org/10.1016/j.dt.2020.04.014

[24] Husain Mehdi, R.S. Mishra, Influence of Friction Stir Processing on Weld Temperature Distribution and Mechanical Properties of TIG-Welded Joint of AA6061 and AA7075. Transactions of the Indian Institute of Metals, 73, 1773–1788 (2020). https://doi.org/10.1007/s12666-020-01994-w

[25] X. Zhang, S.F. Li, D. Pan, B. Pan, K. Kondoh, Microstructure and synergistic- strengthening efficiency of CNTs-SiC dual-nano reinforcements in aluminum matrix composites, Compos. Appl. Sci. Manuf. 105 (2018) 87–96.

[26] Alidokht SA, Abdollah-zadeh A, Soleymani S, Assadi H. Microstructure and tribological performance of an aluminium alloy based hybrid compositeproduced by friction stir processing. Mater Des 2011;32:2727–33.

[27] Husain Mehdi, Sipokazi Mabuwa, Velaphi Msomi, Kuldeep kumar Yadav, Influence of Friction Stir Processing on the Mechanical and Microstructure Characterization of Single and Double V-Groove Tungsten Inert Gas Welded Dissimilar Aluminum Joints. Journal of Materials Engineering and Performance (2022). https://doi.org/10.1007/s11665-022-07659-7.

[28] Sharifitabar M, Sarani A, Khorshahian S, Shafiee Afarani M. Fabrication of5052Al/Al2Onanoceramic particle reinforced composite via friction stir processing route. Mater Des 2011;32:4164–72.3

[29] A.Nait Salah, Husain Mehdi, Arshad Mehmood, Abdul Wahab Hashmid, Chandrabhanu Malla, Ravi Kumar, Optimization of process parameters of friction stir welded joints of dissimilar aluminum alloys AA3003 and AA6061 by RSM, Materials Today: Proceedings, 56 (4), 1675-1684, 2021, https://doi.org/10.1016/j.matpr.2021.10.288.

[30] Husain Mehdi, R.S. Mishra, R.S. Analysis of Material Flow and Heat Transfer in Reverse Dual Rotation Friction Stir Welding: A Review, International Journal of Steel Structures, 19, 422–434 (2019). https://doi.org/10.1007/s13296-018-0131-x.

[31] Feng AH, Xiao BL, Ma ZY. Effect of microstructural evolution on mechanical properties of friction stir welded AA2009/SiC composite. Compos Sci Technol 2008;68:2141–8.

[32] Uzun H. Friction stir welding of SiC particulate reinforced AA2124 aluminium alloy matrix composite. Mater Des 2007;28:1440–6.

[33] Husain Mehdi, R.S. Mishra, An experimental analysis and optimization of process parameters of AA6061 and AA7075 welded joint by TIG+FSP welding using RSM, Advances in Materials and Processing Technologies, 8(1), 598-620, 2022. https://doi.org/10.1080/2374068X.2020.1829952.

[34] Sun K, Shi QY, Sun YJ, et al.. Microstructure and mechanical property of nano-SiC strength Mg bulk composites produced by friction stir processing. Mater Sci Eng A 2012; 547: 32-37.

[35] Marzoli L M, Strombeck A V, Dos Santos J F, Gambaro C, and Volpone L M, Friction stir welding of an AA6061/Al2O3/20p reinforced alloy, Compos Sci Technol 66 (2006) 363-371.

[36] Husain Mehdi, R.S. Mishra, Effect of Friction Stir Processing on Mechanical Properties and Wear Resistance of Tungsten Inert Gas Welded Joint of Dissimilar Aluminum Alloys. Journal of Materials Engineering and Performance volume, 30, 1926–1937 (2021). https://doi.org/10.1007/s11665-021-05549-y.

[37] Z.Y.Zhanga, R. Yang, Y.Lia, G.Chena, Y.T.Zhao, M.P.Liu, Microstructural evolution and mechanical properties of friction stir processed ZrB2/6061Al nanocomposites, Journal of Alloys and Compounds, 762, 312-318, 2018.

[38] Husain Mehdi, R.S. Mishra, Consequence of reinforced SiC particles on microstructural and mechanical properties of AA6061 surface composites by multi-pass FSP, Journal of Adhesion Science and Technology, 36(12), 1279-1298, 2022, https://doi.org/10.1080/01694243.2021.1964846.

[39] Chen X G, Silva M D, Gougeon P, and St-Georges L, Microstructure and mechanical properties of friction stir welded AA6063–B4C metal matrix composites, Mater Sci Eng A 518 (2009) 174-184.

[40] Vijay S J, and Murugan N, Influence of tool pin profile on the metallurgical and mechanical properties of friction stir welded Al–10 wt.% TiB2 metal matrix composite, Mater Des 31 (2010) 3585-3589.

[41] Nami H, Adgi H, Sharifitabar M, and Shamabadi H, Microstructure and mechanical properties of friction stir welded Al/Mg2Si metal matrix cast composite, Mater Des 32 (2010) 976-983.

[42] Husain Mehdi, R.S. Mishra, Microstructure and mechanical characterization of tungsten inert gas-welded joint of AA6061 and AA7075 by friction stir processing, Proceedings of the Institution of Mechanical Engineers, Part L: Journal of Materials: Design and

Applications, 235 (11), 2531-2546 (2021), https://doi.org/10.1177/14644207211007882.

[43] H.A. Deore, J. Mishra, A.G. Rao, H. Mehtani, V.D. Hiwarkar, Effect of filler material and post process ageing treatment on microstructure, mechanical properties and wear behaviour of friction stir processed AA 7075 surface composites, Surf. Coat. Technol 374 (2019) 52–64.

[44] Yuming Xie, Xiangchen Meng, Yulong Li, Dongxin Mao, Long Wan, Yongxian Huang, Insight into ultra-refined grains of aluminum matrix composites via deformation-driven metallurgy, Composites Communications 26 (2021) 100776.

[45] Husain Mehdi, R.S. Mishra, Effect of multi-pass friction stir processing and SiC nanoparticles on microstructure and mechanical properties of AA6082-T6, Advances in Industrial and Manufacturing Engineering, 3, 100062 (2021). https://doi.org/10.1016/j.aime.2021.100062

[46] A.Nait Salah, M. Kaddami, Husain Mehdi, Mechanical Properties And Microstructure Characterization of Friction Stir Welded Joint Of Dissimilar Aluminum Alloy AA2024 And AA7050, Turkish Journal of Computer and Mathematics Education, 12(7), 1051-1061 (2021).

[47] Husain Mehdi, R.S. Mishra, Modification of Microstructure and Mechanical Properties of AA6082/ZrB2 Processed by Multipass Friction Stir Processing. Journal of Materials Engineering and Performance, 32, 285–295 (2023). https://doi.org/10.1007/s11665-022-07080-0.

[48] El-Rayes, M.M., El-Danaf, E., 2012. The influence of multi-pass friction stir processing on the microstructural and mechanical properties of Aluminum Alloy 6082, J Mater Process Tech. 212, 1157–1168.

[49] A. Sharma, V.M. Sharma, S. Mewar, S.K. Pal, J. Paul, Friction stir processing of Al6061-SiC-graphite hybrid surface composites, Mater. Manuf. Process. 33 (7) (2018) 795–804.

[50] Husain Mehdi, Shwetanshu Gaurav, Teetu Kumar, Prasoon Sharma, Mechanical Characterization of SA-508Gr3 and SS-304L Steel Weldments, International Journal of Advanced Production and Industrial Engineering, 2(1), 41-46, 2017.

[51] M. Paidar M, O.O. Ojo, H.R. Ezatpour, A. Heidarzadeh, Influence of multi-pass FSP on the microstructure, mechanical properties and tribological characterization of Al/B C composite fabricated by accumulative roll bonding (ARB), Surf. Coating. Technol. 361 (2019) 159–169.

[52] Preety Rani, R.S. Mishra, Husain Mehdi, Effect of Nano-sized Al2O3 particles on microstructure and mechanical properties of aluminum matrix composite fabricated by multipass FSW, Part C: Journal of Mechanical Engineering Science (SAGE), 2022. https://doi.org/10.1177/09544062221110822.

[53] J.Q. Su, T.W. Nelson, R. Mishra, M. Mahoney, Microstructural investigation friction stir welded 7050-T651 aluminium, Acta Mater. 51 (2003) 713-729.

[54] Husain Mehdi, Rajan Upadhyay, Rohan Mehra, Adit Singhal, Modal Analysis of Composite Beam Reinforced by Aluminium-Synthetic Fibers with and without Multiple Cracks Using ANSYS, International Journal of Mechanical Engineering, 4(2), 2014, 70-80.

[55] L.B. Johannes, R.S. Mishra, Multiple passes of friction stir processing for the creation of superplastic 7075 aluminum, Mater. Sci. Eng., A 464 (1) (2007) 255–260.

[56] Naman Sharma Husain Mehdi, Shivam Sharma, Mohd Anas, The Influences of Variation of Copper Content on the Mechanical Properties of Aluminium Alloy, International Journal of Material Science Innovations, 3(3), 2015, 74-86.

[57] Heidarzadeh, A., Barenji, R.V., Esmaily, M., Ilkhichi, A.R., 2015. Tensile Properties of Friction Stir Welds of AA 7020 Aluminum Alloy, Trans. Indian Inst. Met. 68, 757–767.

[58] Liu, H.J., Fujii, H., Maeda, M., Nogi, K., 2013. Tensile properties and fracture locations of friction-stir-welded joints of 2017-T351 aluminum alloy, J Mat. Proc. Technol, 142, 692–696.

[59] Huang KT, Lui TS, Chen LH. Effect of microstructural feature on the tensile properties and vibration fracture resistance of friction stirred 5083 alloy. J Alloys Compd. 2011;509(27):7466.

[60] S.S. Mirjavadi, M. Alipour, A.M.S. Hamouda, A. Matin, S. Kord, B.M. Afshari, P.G. Koppad, Effect of multi-pass friction stir processing on the microstructure, mechanical and wear properties of AA5083/ZrO_2 nanocomposites, J. Alloys Compd. 726 (2017) 1262–1273.

[61] Manoj Saini, Navneet Arora, Chandan Pandey, Husain Mehdi, Preliminary studies on thermal cycling of reactor pressure vessel steel, International Journal of Mechanical Engineering, 4(2), 2014, 51-58.

[62] F. Khodabakhshi, M. Haghshenas, J. Chen, B. Shalchi Amirkhiz, J. Li, A.P. Gerlich, Bonding mechanism and interface characterisation during dissimilar friction stir welding of an aluminium/polymer bi-material joint, Sci. Technol. Weld. Join. 22 (2017) 182–190.

[63] Middling, O.T., Oosterkamp, L.D., Bersaas, J., 1998. Friction stir welding aluminium process and applications. Int: Proc.7 Inter. conf. jt. alum., INALCO98.

[64] F.J. Humphreys, M. Hatherly, Chapter 11 - grain growth following recrystallization, in: Recrystallization and Related Annealing Phenomena, Elsevier Ltd., 2004, pp. 333–378.

***Cite this article as**:* Vikas Kumar, Promila, Amit Gupta, Effect of nanoparticles and multipass friction stir processing on microstructure and mechanical properties of AA7475 International Journal of Research in Engineering and Innovation Vol-7, Issue-3 (2023), 94-101. *https://doi.org/10.36037/IJREI.2023.7301*.